

SPIDER high voltage bushings: Design, development and first experimental tests

N. Pilan^{a,*}, L. Grandò^a, A. De Lorenzi^a, A. Masiello^b, C. Lievin^c

^a Consorzio RFX, Corso Stati Uniti 4, I-35127 Padova, Italy

^b Fusion for Energy F4E, Barcelona, Spain

^c THALES ELECTRON DEVICES, 2 rue Marcel Dassault – BP 23 78141, Vélizy-Villacoublay Cedex, France

HIGHLIGHTS

- A thorough R&D activity on the SPIDER High Voltage Bushing has been carried out.
- The design has been numerically verified considering the voltage holding issues.
- The experimental validation has been successfully completed.

ARTICLE INFO

Article history:

Received 19 September 2016

Received in revised form 19 January 2017

Accepted 3 April 2017

Available online xxx

Keywords:

Insulator
High voltage
Ceramic
Vacuum
Electrostatic accelerator

ABSTRACT

The ITER project requires at least two Neutral Beam Injectors (NBIs), each accelerating to 1 MV a 40A beam of negative deuterium ions, to deliver to the plasma a power of about 33 MW for one hour as additional heating. The fulfilment of such demanding performances required the realization of the full size prototype of the negative ion source (SPIDER – Source for Production of Ion of Deuterium Extracted from RF plasma), as well as the full size prototype of the whole 1 MV ITER injector (MITICA – Megavolt ITER Injector & Concept Advancement) at PRIMA, the test facility for the ITER neutral beams now under construction at the Consorzio RFX in Padua, Italy.

The SPIDER plasma source- housed in a stainless steel vessel maintained in high vacuum – is polarized at 112 kV (12 kV extraction voltage and 100 kV accelerating voltage), so that the vacuum vessel must be equipped with three large alumina feedthroughs, ring shaped insulators (820 mm in diameter) necessary to supply the electric, hydraulics gas and diagnostic services to the plasma source. These insulators (bushings) belong to the most critical items in the SPIDER assembly and they required a particular effort in designing, manufacturing and testing. This paper gives an overview of the insulator design, development, manufacturing activities and presents the results of the high voltage acceptance tests.

© 2017 Elsevier B.V. All rights reserved.

1. Introduction

The need of plasma heating and control in fusion power plants directs the R&D of Neutral Beam Injectors (NBI) toward high energy, high power and long pulse operations.

The present concept for the high power negative ion NBI in ITER is based on a linear electrostatic accelerator and a gas neutralizer. Several papers are available dealing with working principles, engineering issues, technical solutions, and design details [1].

One of the most challenging aspects of the NBI for ITER is the direct exposure of the Beam Source (BS) to the radiation coming

from the reactor due to neutrons and gamma rays [2–6]. Such exposure causes the Radiation Induced Conductivity (RIC) phenomena in insulating gases, so that in ITER NBI the insulation of the BS to the ground is obtained only by vacuum insulation [2]. This is the reason why in SPIDER it has been chosen vacuum as insulating media.

This design choice has implied the introduction of a remarkable change in the injector lay-out with respect to the injectors so far developed. As a consequence, a number of issues regarding the voltage holding in vacuum needed to be solved, especially as far as the feedthroughs are concerned.

2. Overall design description

The BS of SPIDER is electrically insulated from the vacuum vessel by four post insulators which transfer the weight of the whole

* Corresponding author.

E-mail address: nicola.pilan@igi.cnr.it (N. Pilan).

source to the bottom part of the vacuum vessel. One of the main issues relevant to the insulation was the coolant supply to the source. Two possibilities have been analyzed and compared in term of pros and cons.

The first and most straightforward solution, shown in the sketch of Fig. 1 “Case A”, foresees the adoption of a single feedthrough and a single insulating pipe respectively for each electrical and cooling line going to the BS. In this solution all the feedthroughs (24 lines) and all the cooling pipes (21 lines) shall be rated for the maximum voltage (112 kV). The main drawback of solution “A” is the too short length L of the insulating breaks carrying the cooling water. This length L (< 0.7 m) is determined by the vacuum vessel and BS dimensions; in fact, the pipes material must be ceramic, because it has to be compatible with vacuum and to have adequate mechanical characteristics. For this reason, the pipes must be straight, any bend is not allowed

The ultrapure water adopted in the cooling circuit has resistivity in the range 1–5 MOhm*cm (depending on water temperature, pH, and foreign ions concentration).

The total current drain expected at nominal voltage for the solution case “A” is of the order of some hundreds of mA: such a high current can cause water hydrolysis and unacceptable galvanic corrosions at the interfaces between metal and insulating materials. Moreover solution case “A” requires a high number of expensive air-vacuum electrical feedthroughs (most of them not off the shelf components) so a specific R&D would be necessary.

The alternative solution shown in Fig. 1 “Case B” consist of three bushings (highlighted in red) the upper one dedicated to the electrical lines, the bottom ones dedicated to the cooling circuits and to the gas lines.

Solution “B” includes a set of insulating breaks, in air-side, each break having length L' . Thus the length of the breaks is not limited by the vacuum vessel dimension and it is possible to reduce the current drained by the insulating water by extending the break lengths $L' \gg L$.

Moreover, considering that the insulating pipes must deliver hot water at a temperature ranging from 30 to 180 °C with a nominal pressure of 25 bar, we notice that solution “B” has also the advantage that metallic pipes can be used in the vacuum section and commercial pipes made of Teflon reinforced by a Kevlar® braid can be used in the air section. Instead, according to Solution “A” such high demanding requirements are difficult to be met by a single type of flexible, insulating, vacuum-compliant pipe.

In Fig. 2 it is shown a detailed cross section of the bushing on the top of the vessel. The vacuum gap length between the central screen made of stainless steel and the vacuum vessel is 67 mm.

The external surfaces of the ceramics are exposed to the atmospheric air while the internal surfaces are in high vacuum with a pressure ranging from 10^{-7} mbar to 5×10^{-4} mbar. A stainless steel flange, polarized at the BS potential, closes each ceramic ring. A Viton gasket, between ceramic and stainless steel, prevents the leak of atmospheric air in the vacuum vessel. The same structure has been adopted both for the electric and for the hydraulic bushings. The ceramic insulator of each bushing is a ring of sintered high purity alumina (concentration of $\text{Al}_2\text{O}_3 > 99\%$), outer diameter 820 mm, inner diameter 702 mm, high 300 mm. A set of 12 blind threaded holes M12 have been done on the flat surfaces of the sintered ceramic to join the bushing to the other metallic parts.

The bottom surface of each threaded hole has been metalized to prevent the occurrence of partial discharges in the trapped volume between the metallic screw and the blind hole.

A central metallic screen, 506 mm in diameter, polarized at the BS potential, surrounds the BS conductors in the upper bushing (see Fig. 2); the same type of screen surrounds respectively the inlet and

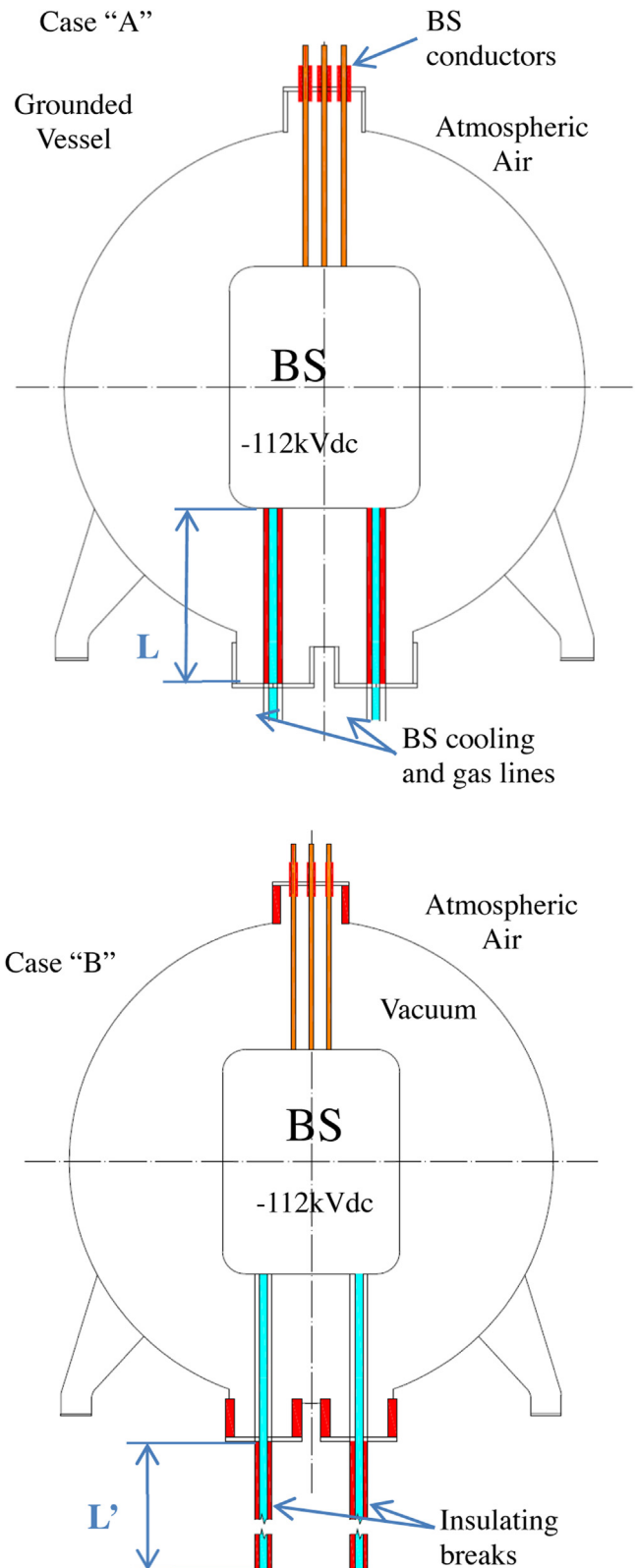


Fig. 1. Sketch of alternative lay-outs. Insulators, cooling water lines and BS conductors are represented respectively in red, cyan and orange. (For interpretation of the references to colour in this figure legend, the reader is referred to the web version of this article.)

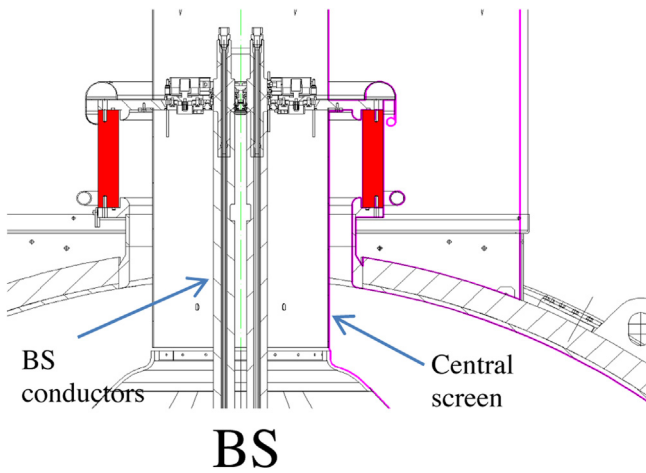


Fig. 2. View of SPIDER upper HV bushing, showing the cross-section of vacuum vessel, ceramic bushing and BS screen. The boundaries of the Finite Element Model used for electric field calculation are shown in magenta, the ceramic material, is shown in red.

the outlet BS cooling lines in the bushing located in the bottom part of the vacuum vessel.

3. Finite element analyses and electrostatic verifications

Electrostatic analyses have been performed considering the domain highlighted by magenta lines in Fig. 2. The analyses are representative both of the hydraulic and the electrical bushing. The inner volume inside the central conductor is not included in the domain of the simulation (no electric field inside).

The electrostatic field distribution has been calculated solving the Poisson’s equation for the dielectric materials, the relative permittivity ϵ_r of the alumina rings is 9.6.

In Fig. 3 it is shown the electrostatic field map at nominal voltage (–112 kV). The maximum electric field in vacuum is 2.4 kV/mm on the anodic surface of the vacuum vessel, while the maximum elec-

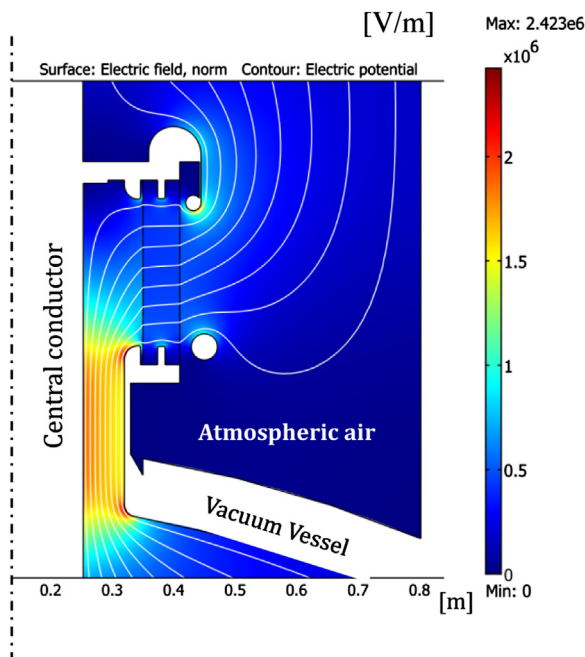


Fig. 3. Electrostatic field map, Electric field modulus at nominal voltage (–112 kV), Minimum distance between central conductor and Vacuum Vessel 67 mm.

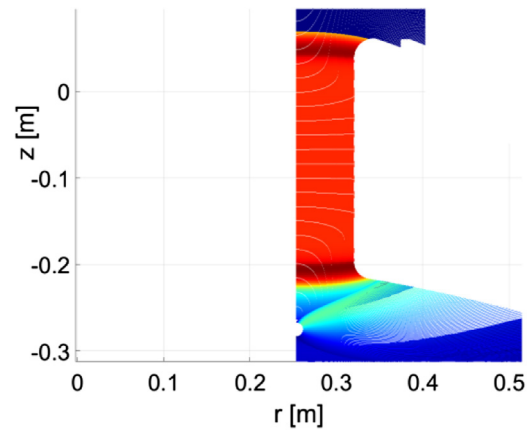


Fig. 4. Calculated distribution of negative particles trajectories leaving from the cathode surfaces. The warmer the color the higher is the breakdown probability corresponding to each trajectory.

tric field in air is 1.8 kV/mm, it is on the bottom part of the screen at the cathode side. The bushing was designed according with the criteria reported in table 1 of [7], the following limits of electric field have been considered: 4, 1, 0.1 kV/mm respectively for: metal surfaces (with voltages <200 kV), insulator surfaces and cathode triple points. The dielectric strength of the solid (high purity) alumina is 17 kV/mm, which is about one order of magnitude higher than calculated.

Further numerical analyses were carried out after the first experimental tests by using a recently developed predictive code [7], which allows to calculate the breakdown probability of a system insulated by large vacuum gaps.

The region having the higher breakdown probability in vacuum is between the central conductor and the vacuum vessel, the minimum gap length is 67 mm. Fig. 4 shows the trajectories of the negative particles leaving from the cathode surfaces, as calculated using the predictive code.

The breakdown probability of the sole vacuum gap, between the central conductor and the vacuum vessel has been calculated by using the Weibull parameters $W_0 = 1.15e16 [V^{8/3}/m^{5/3}]$ and $m=8$ reported in [8]. The results are shown in Fig. 5, the cumulative BreakDown (BD) probability is function of the BD Voltage at the end of the conditioning procedure in high vacuum ($p < 10^{-06}$ – 10^{-05} mbar).

The probabilistic model highlights a breakdown voltage associated to the vacuum gap (67 mm in length) in the range of 150–200 kVdc. Therefore, the above described numerical analyses and the adopted design criteria, based on the cumulative breakdown probability, have confirmed that no particular issues is expected for the operation of the proposed geometry at the nominal accelerating voltage.

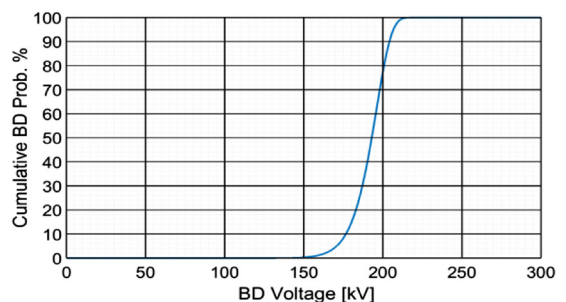


Fig. 5. Cumulative breakdown probability vs. applied voltage for the detail shown in Fig. 4.

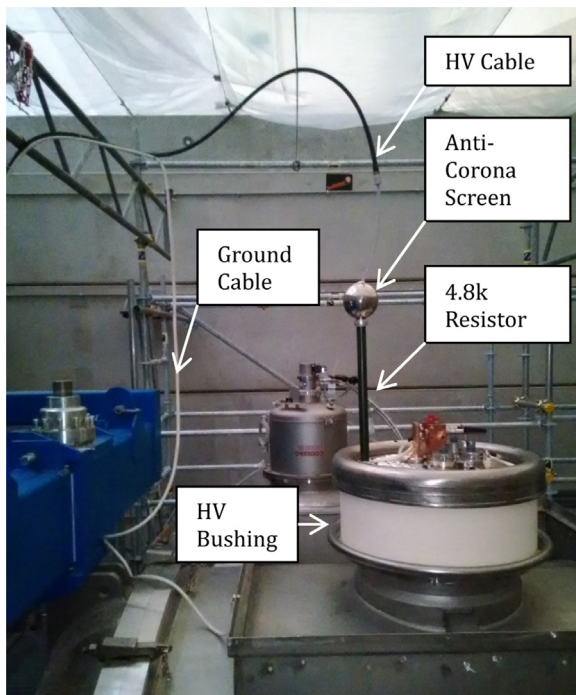


Fig. 6. Experimental set-up of the high voltage endurance tests.

4. First high voltage tests on site

High voltage tests on the bushing prototypes were performed with the setup shown in Fig. 6. A high voltage Cockcroft-Walton DC Power Supply (PS), negative polarity, was connected to each bushing flange by the High Voltage cable shown in Fig. 6. A high voltage resistor of 4.8kOhm was inserted between the PS and the bushing flange to limit the breakdown current during the high voltage conditioning procedure [9]. The high voltage cable has an equivalent capacitance of 1nF, while the HV bushing has an equivalent capacitance of 0.12 nF.

The target was sustain 120kV without breakdown for at least 3 h. The first test was not successful; micro-discharges [10] started at about 65 kV and it was not possible to reach a voltage higher than 80kV. The vacuum vessel and the central conductor were cleaned and some sharp edges due to the presence of screws were removed from the central conductors. The high voltage test was repeated: the conditioning history is shown in Fig. 7 in term of applied voltage and drained current as function of the HV application time. During

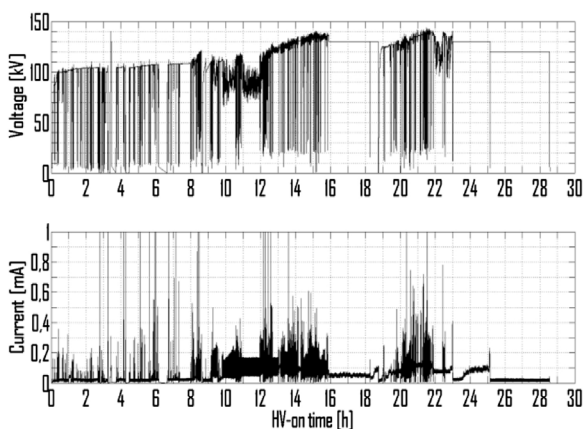


Fig. 7. High Voltage endurance test records. A) Voltage vs. HV on time. B) Drain Current vs HV application time.

the execution of test many breakdowns were observed. Moreover the occurrence of many microdischarges has been recorded in term of spikes of currents, fluctuation of pressure, and presence of X rays. The first micro discharges occurred at about 95 kV shown a clear improvement of the voltage holding capability. The sole high voltage cable was tested at $t = 3$ h up to 140 kV for few minutes to exclude issues in the setup.

After about 15 h of conditioning at increasing voltage levels, the first long duration test at 130 kV was carried out successfully; the voltage was sustained for 2 h 25'. After additional conditioning, a second long duration test was also carried out at 130 kV for 2 h and 6 min; the current was lower than 50 μ A. In both cases the endurance tests at 130 kV were carried out after increasing the voltage up to 136 kV to assure a certain margin against some possible breakdowns which can inevitably occur at this high voltage levels. The last long duration test was done at 120 kV; the voltage has been sustaining for 3 h 20' without breakdowns.

5. Conclusions

The large HV ceramic bushing for SPIDER has been successfully developed through careful design, realization and testing. The experience gained so far has allowed to better understand the intrinsic critical points and the limits of the system in term of voltage holding performances. On the basis of the final tests, these limits resulted well consistent with the target voltage holding level for which the system has been designed.

Acknowledgments

The project has been funded with support from Fusion for Energy. This publication reflects the views only of the author, and Fusion for Energy cannot be held responsible for any use which may be made of the information contained therein. The views and opinions expressed herein do not necessarily reflect those of the ITER Organization

References

- [1] V. Toigo, et al., Progress in the realization of the PRIMA neutral beam test facility, Nucl. Fusion 55 (083025) (2015) 2.
- [2] R.S. Hemsworth, et al., Neutral beams for ITER, Rev. Sci. Instrum. 67 (1996) 1120–1125.
- [3] P.L. Mondino, et al., ITER neutral beam system, Nucl. Fusion 40 (501) (2000).
- [4] T. Inoue, et al., Radiation Analysis of the ITER neutral beam system, Proc. 20th SOFT Marseille (1998).
- [5] E. Hodgson, et al., Radiation induced power loss in insulating gases for ITER NBI systems, Proc. 20th SOFT Marseille (1998).
- [6] Y. Fujiwara, et al., Experimental study on the influence of radiation on high-voltage insulation gases, JAERI tech. Report 99-071, 1999.
- [7] A. Masiello, Adaptation of the 1 MV bushing to the SINGAP concept for the ITER NB injector test bed, Nucl. Fusion 46 (2006) S340.
- [8] N. Pilan, P. Veltri, A. De Lorenzi, Voltage holding prediction in multi electrode?multi voltage systems insulated in vacuum, IEEE Trans. Dielectr. Electr. Insul. 18 (2) (2011).
- [9] M. Boldrin, et al., The transmission line for the SPIDER experiment, Fusion Eng. Des. 86 (2011) 754.
- [10] P. Spolaore, et al., The large gap case for HV insulation in vacuum, IEEE Trans. Dielectr. Electr. Insul. 4 (4) (1997).